Super-resolution microscopy demystified

Lothar Schermelleh[1,*], Alexia Loynton-Ferrand[2], Thomas Huser[3], Christian Eggeling[4,5], Markus Sauer[6], Oliver Biehlmaier[2], Gregor P. C. Drummen[7,8,*]

[1] Micron Oxford Advanced Bioimaging Unit, Department of Biochemistry, University of Oxford, Oxford, UK
[2] Imaging Core Facility, Biozentrum, University of Basel, Basel, Switzerland
[3] Biomolecular Photonics, Department of Physics, University of Bielefeld, Bielefeld, Germany
[4] MRC Human Immunology Unit and Wolfson Imaging Centre Oxford, Weatherall Institute of Molecular Medicine, University of Oxford, Oxford, UK.
[5] Institute for Applied Optics, Friedrich-Schiller-University Jena & Leibniz Institute of Photonic Technology, Jena, Germany
[6] Department of Biotechnology & Biophysics, Biocenter, Julius Maximilian University of Würzburg, Würzburg, Germany
[7] Advanced Bio-Imaging Program, Bio&Nano Solutions–LAB[3]BIO, Bielefeld, Germany
[8] ICON-Europe.org, Exxilon Scientific Events, Steinhagen, Germany

*Correspondence to L.S. and G.D.: lothar.schermelleh@bioch.ox.ac.uk; gpcdrummen@bionano-solutions.de

Author contributions

L.S., A.F. and G.D. provided the initial concept, design and drafting of the manuscript with contributions of all authors. L.S. and G.D. prepared figures. L.S., T.H and G.D. revised, and finalized the manuscript. All authors read and approved the final version of the manuscript.

Conflicts of interest

G.D. is partially exempted from his duties at BNS to pursue fundamental scientific research. The authors declare no further conflicts of interest.

Keywords

Super-resolution microscopy, optical nanoscopy, single molecule localization microscopy, structured illumination microscopy, stimulated emission depletion microscopy, confocal microscopy, expansion microscopy, lattice light sheet, spatial resolution, diffraction limit, photoswitching, cellular dynamics, deep learning

Abstract

Super-resolution microscopy (SRM) bypasses the diffraction limit, a physical barrier that restricts the optical resolution to roughly 250 nm and was previously thought to be impenetrable. SRM techniques allow the visualization of subcellular organization with unprecedented detail, but also confront biologists with the challenge of selecting the best-suited approach for their particular research question. Here, we provide guidance on how to use SRM techniques advantageously for investigating cellular structures and dynamics to promote new discoveries.

Introduction

In their pursuit to understand cellular function, biologists seek to observe the processes that allow cells to maintain homeostasis and to react dynamically to internal and external cues, on a molecular scale and inside structurally intact, ideally living specimens. A pathway towards this goal was opened with the advent and widespread application of super-resolution microscopy (SRM) techniques that manage to surpass the 'classical' diffraction limit of optical resolution of about half the wavelength of the emitted light[1]. These fluorescence microscopy techniques are continuously pushing the resolution barrier towards nanometre scales, thereby enabling the imaging of cellular structures with a level of detail that was previously only achievable with electron microscopy (EM). At the same time SRM techniques retain the advantages of optical microscopy with regard to sample preservation, imaging flexibility and target specificity. SRM allows the extraction of quantitative information on spatial distributions and often also absolute numbers of proteins or other macromolecules within subcellular compartments. SRM can also reveal three-dimensional (3D) structural details, and provides direct experimental feedback for modelling complex biological interactions[2].

SRM systems are now commercially available and a growing number of institutional core facilities offer advanced imaging. However, the field has grown so rapidly that biologists can easily be overwhelmed by the vast range of SRM variants. For the less experienced user, choosing the SRM technique that is best suited to address a particular biological question has become increasingly complicated and resulted in various misconceptions. This review is tailored to biological users with less experience in SRM and intends to provide a concise overview of commercially available and emerging SRM techniques together with a balanced assessment of their strengths and weaknesses with biological applications in mind. Further-reaching technical and historical information on SRM can be found elsewhere[2-7]. Here, we seek to strike a balance between sharing our excitement for the opportunities provided by SRM, and managing expectations in order to guide decision-making on how to incorporate SRM into particular fields of research.

An overview of SRM methods

Current SRM methods are based either on wide-field (WF), total internal reflection fluorescence (TIRF) or confocal microscope setups (Fig. 1a-c) and fundamentally differ in how fluorescently labelled samples are excited and how the emitted photons are detected (Fig. 1d-h; Box 1). One group of SRM techniques falls under super-resolution structured illumination microscopy (SR-SIM, reviewed in[7,8]) and comprise traditional interference-based linear 2D and 3D SIM[9-11] (Fig. 1d) as well as more recently introduced point scanning SIM approaches[12-15] (Fig. 1e). Even though they exceed the 'classical' Abbe limit of resolution, SR-SIM approaches are still fundamentally bound by the laws of diffraction, at best doubling the spatial resolution in lateral (x, y) and axial (z) directions, equivalent to an ~8-fold volumetric improvement. By renouncing higher resolution and its concomitant demands and restrictions, SR-SIM methods are considered rather 'gentle' and are particularly geared towards live-cell imaging and higher throughput applications. Classic interference-based SIM utilizes frequency shifting upon patterned wide-field illumination and mathematical reconstruction, reaching 100 nm lateral and 300 nm axial resolution with standard high numerical aperture (NA) objectives (Fig. 1d; Box1). By relying on sensitive camera detection, the approach is very photon-efficient, allows routine imaging with multiple colours and conventional fluorophores, and is well suited for volumetric live-cell imaging[16,17]. On the downside, classic interference-based SIM requires mathematical post-processing and a carefully aligned and

calibrated microscope setup, bearing an increased risk of reconstruction artifacts, which require significant knowledge to detect and counteract[18].

Illumination by a focused spot and confocal detection is a different way of generating 'structured illumination'. However, in standard single point laser scanning or multi-point spinning disc confocal setups, the ability to increase resolution is dampened by noise and low throughput of high-frequency information due to signal rejection. More recently, effective methods have been developed and commercialized based on single point-scanning (Re-scan, Airyscan) or multi-point scanning (instant SIM) principles that employ fast multipixel detectors to offset signal loss of smaller pinhole sizes (Fig. 1e). Using a robust deconvolution reconstruction approach with reduced risk of artifacts, these approaches realize up to 1.7-fold improvement in lateral resolution and ~5-fold improvement in volumetric resolution[12,15,19]. As readily available extensions to existing top-end confocal systems, they require only little adaptation in terms of sample preparation and have become a popular entry level choice to SRM. Interference-based SR-SIM not only provides slightly higher (3D) resolution, but also delivers higher signal-to-noise ratio at high spatial frequencies and superior optical sectioning in thin samples. In contrast, point scanning SIM methods perform better with thicker and densely labelled samples due to efficient background filtering prior to image formation[8]. Moreover, both high-speed interference pattern generation and parallelized detection in multi-point scanning implementations provide unrivalled acquisition speed for live-cell SRM applications[14,15,20].

In contrast to SR-SIM, diffraction-unlimited SRM techniques are theoretically able to push resolution levels down to infinitesimally small scales. In reality, however, experimental constraints such as high irradiation intensities, labelling density and prolonged imaging times constrain the achievable resolution, especially in live-cell experiments. Their unifying basic principle is to exploit the modulation or switching of fluorescence emission. Also referred to as nanoscopy, this group can be subdivided into targeted (or deterministic) approaches that use directed focused laser beams for on/off-switching, and stochastic approaches that use wide-field illumination for random on/off-switching and subsequent algorithmic event detection and image reconstruction.

The most common targeted approach is stimulated emission depletion (STED) microscopy (Fig. 1f; Box 1)[5]. In cells, current commercial STED systems can typically achieve down to 50-60 nm lateral resolution[21]. More recent 3D STED setups also operate along the z-direction, providing the option to freely tune between lateral and axial resolution increase[5]. Being implemented as an add-on modality to standard confocal setups, standard STED is generally considered comparably easy-to-use. Computational post-processing is not required, although additional deconvolution is often applied to compensate for low signal, particularly in samples with increased background. Two-colour imaging is routinely possible with a wide range of fluorophores, but best performance is achieved using dyes with specific properties optimized for STED[22,23], although more channels can be added in conventional confocal mode[5]. The superior lateral resolution of STED microscopy takes particular effect when imaging small, isolated filamentous or vesicular structures with little axial extension, whereas 3D STED is useful for imaging thicker and more densely packed features[5,24]. A unique feature of STED is the tunability of resolution by adjusting the level of laser power (Box 1). This allows weighting spatial resolution against potential photo-damaging effects and thereby enhancing its live-cell imaging capabilities, particularly when combined with customized labels and optimized scanning protocols[5,25]. Alternatively, live-cell imaging can be realized by employing reversibly photoswitchable labels in reversible saturable optical linear fluorescence transitions (RESOLFT) microscopy[5]. A disadvantage shared by all targeted techniques is that reducing the effective

fluorescence observation volume also entails a corresponding decrease in the total signal detected, as well as a decreased scan step size, which increases acquisition time. As with all point scanning methods, imaging speed scales with scan size allowing for very high-frame rates for small imaging windows, whereas imaging entire cells with sufficient photon counts is comparably slow.

The second group of diffraction-unlimited SRMs is based on wide-field illumination and relies on single molecule switching by stochastic excitation and detection of fluorescent point emitters. Collectively termed single molecule localization microscopy (SMLM), these comprise a fairly large number of modalities that are differentiated only by how on/off switching is achieved (Fig. 1g; Box 1). SMLM approaches are very popular, because they can be implemented at low cost on conventional camera-based wide-field setups, shifting the complexity to biological sample preparation and downstream reconstruction and data analysis. Most SMLM implementations can separate individual dyes with distances reduced to 20 nm lateral and 50 nm axial resolution. The precision of determining the centroid position of a fluorescent signal depends mainly on the photon count (~ (number of photons detected)$^{1/2}$). However, structural resolution, for example the ability to distinguish biological features such as filaments, depends on the sample's labelling density and switching properties [2,26,27]. As a general rule, achieving a specific structural resolution, requires that the distance between neighbouring localizations be at least 2-fold smaller to meet the Nyquist sampling criterion[28-30].

Detection efficiency and signal-to-background ratio can be improved significantly by combination with TIRF or highly inclined and laminated optical sheet (HILO) illumination[31]. Disadvantages of SMLM arise from the complexity of the image reconstruction process, which requires careful consideration of falsely identified or localized individual emitters, e.g. due to high label densities or inappropriately set photoswitching rates[32]. Further requirements include either specifically photoswitchable or -activatable fluorescent labels (e.g. (fluorescence) photo activation localization microscopy ((f)PALM)) and special buffer conditions to induce blinking of conventional dyes (e.g. (direct) stochastic optical reconstruction microscopy ((d)STORM))[33,34]. The necessity to acquire thousands of camera frames to reconstruct a single plane and the associated lengthy acquisition time restricts the general applicability of SMLM for live-cell imaging. As for all SRM methods, in order to avoid artefacts the acquisition time should be shorter than the time it takes for the observed structural feature to move approximately one resolution length. Therefore, only a few examples successfully demonstrated live-cell SMLM[2,26,35-37]. More recently, fluctuation analysis methods, super-resolution optical fluctuation imaging (SOFI[38]) and super-resolution ring correlation (SRRF[39]), enable extracting information from samples exhibiting higher density intermittent fluorescence which occurs at much lower light levels and allows trading optical resolution for temporal resolution required for live-cell recordings. In addition, using photoswitching and localization, the SMLM-based recording scheme also allows quantitation of local molecular diffusion and interaction dynamics in densely labelled living cells via single-molecule tracking[40].

A shortcoming of all imaging approaches discussed above is that they use the same objective lens to excite and detect fluorescence. As a consequence of this epi-illumination (TIRF is a notable exception) areas below and above the image plane are also excited causing additional phototoxicity and generating unwanted out-of-focus signal that is detrimental to image contrast. Light-sheet fluorescence microscopy avoids these effects by exciting fluorophores perpendicular to the sample through a separate low NA objective lens. Although essentially limited to conventional resolution, it is characterized by very high imaging speed, high signal-to-noise ratio, and good optical penetration depth, rendering light sheet microscopy particularly beneficial for *in vivo* imaging of small organisms

or embryos[41]. Bessel beam illumination[42] and the more recently introduced lattice light sheet (LLS) microscopy[43] (Fig. 1h) expand this principle to achieve a close to isotropic resolution of 230 x 230 x 370 nm, thus improving the volumetric resolution of conventional 3D imaging. Further resolution increase can be achieved by combination with SIM[43,44]. LLS allows whole cell volumetric imaging with unrivalled spatiotemporal resolution, but at the expense of fairly complex multi-objective setups and in a confined sample space that requires expert handling.

Finally, expansion microscopy (ExM) provides an ingenious way of obtaining non-optical super-resolution by physical expansion of the specimen. Here, fluorophores of a labelled specimen are fixed to a polymer matrix, which is then allowed to swell in all dimensions in a highly controlled manner[45,46]. ExM requires no special equipment other than a conventional microscope and is possible using standard dyes and antibodies[46], in cells and tissues and is suitable for routine clinical applications [47]. Still, each new application of ExM needs specific optimization. The introduction of iterative ExM[48], which achieves ~20 times expansion of samples, as well as the combination with SIM[49,50] are recent improved developments, although the highly invasive sample treatment prohibits its use in dynamic or live imaging applications.

Experimental design and labelling

Any imaging technique is ultimately defeated by lack of contrast[51]. Therefore, progress in SRM is closely interlinked with the development and best use of biologically compatible fluorescent labels[52-57]. For live-cell imaging, genetically fused fluorescent protein (FP) tags are the most common way to label proteins of interest. They are substantially smaller than IgG antibodies with barrel-like structures of 2-5 nm length[58]. Despite many new variants with improved properties, FPs are still inferior to organic dyes in terms of brightness and photostability. Genetically encoded self-modifying protein tags such as Halo-Tag or SNAP-tag in conjunction with novel cell-permeable dyes have expanded the repertoire of live-cell SRM[26,59-62]. Nevertheless, such protein tags can potentially interfere sterically with protein function or influence protein mobility within the cell. Therefore, wild-type functionality of labelled proteins must always be verified *a priori*. Alternatively, cellular organelles or the cytoskeleton may also be stained by membrane-permeable dyes specifically binding to these structures[60,63]. Novel membrane probes have also been developed for super-resolution imaging of plasma membrane, endoplasmic reticulum and mitochondria[37]. For fixed cells, indirect immunofluorescence labelling using primary and secondary antibodies is commonly used. Direct labelling of primary antibodies or small labelled single domain camelid antibody fragments (nanobodies: 12-15 kDa vs 150 kDa for IgG and sizes ~2.5 × 4 nm[64]) permit attaching the fluorophore closer to the protein of interest[64-66]. Furthermore, small bright organic dye-labelled phalloidin and taxol probes can be used to label actin and microtubule filaments in fixed cells[67,68]. Click chemistry provides the most direct method to attach an organic dye site-specifically to a protein[69] or to modified precursors of DNA/RNA synthesis. However, fixation protocols need to be optimized for different applications to avoid artefacts[70].

For quantitative SRM of endogenous protein levels, FPs are advantageous because they allow specific stoichiometric labelling of target molecules. However, substituting native proteins with transgenic variants that display wildtype expression and function can be difficult. Therefore, standard immunocytochemistry remains the preferred method for quantitative SRM of endogenous protein levels[71,72] and for labelling posttranslational modifications. Finally, transient on/off binding of fluorescent labels, e.g. through oligonucleotide hybridization in DNA-PAINT (DNA-points accumulation for imaging in nanoscale topography) can be used for SMLM instead of relying on

photophysical transitions, thereby reducing energy load and extending possibilities for multiplexing[71,72].

SRM as a multidimensional challenge

From an optical engineering point, a technique's performance is defined by hard measures, such as the full width at half maximum of the microscope's point spread function (PSF, i.e. the Gaussian-like intensity distribution of small objects in the image), the localization or distance precision of defined calibration targets, or maximum frame rates. In real biological applications, however, photon budget, contrast, and labelling specificity are limiting factors. Low contrast impedes the ability of any imaging technique to achieve its nominal resolution[1,51], and any achieved resolution becomes meaningless if unspecific false-positive signals are detected, or if the observed biological structure is adversely affected by the labelling and/or the imaging process. In fact, there is no all-purpose SRM solution and spatial resolution is only one factor of a much larger equation (Fig. 2).

In general, every increase in optical resolution comes at the expense of more exposures, longer acquisition times, and/or higher energy loads, which conversely decreases temporal resolution and increases photobleaching and phototoxicity[73]. Deepening the information content by adding more dimensions such as multicolour, 3D volumetric and/or time-lapse imaging, is often essential to address a specific biological question. However, this also increases the overall burden to the sample. Consequently, higher resolving techniques require trade-offs, and deciding how best to spend precious photons harvested from a sample is of key importance (Fig. 2). The challenge is to generate sufficient contrast between specific and unspecific photons for a given technique to operate to its capacity. Specimen characteristics play a crucial role. Isolated protein complexes or filaments close to the coverslip are usually unobstructed and well-contrasted, and therefore optimal targets. In contrast, imaging extended structural features or deep within tissue through several cell layers is associated with out-of-focus blur, light scattering, as well as spherical and sample-induced aberrations. Although these problems can be partially compensated by refractive index correction, brighter and more photostable labels and other measures, they cannot be fully addressed.

Thus, venturing into SRM requires a first 'reality check' of the level of resolution that is really needed and at what costs. Ultimately, the biological question should be dictating the SRM choice. If the absolute localization of a single species or the relative location of two species of individual molecules are of utmost interest, but the 3D context and dynamics are less important, then SMLM is a prime choice. Various studies have demonstrated SMLM's ability to obtain quantitative information, e.g., of molecules[71,74] and to resolve molecular structures of isolated macromolecular complexes, such as nuclear pore complexes, by applying particle averaging[75,76]. STED is particularly useful for 2D high-resolution studies of high-contrast targets, such as vesicles, filaments or organelles[77,78] and for deeper imaging in tissues or even living animals[24,79]. STED has proven particularly valuable for deciphering molecular diffusion and interaction dynamics through its combination with fluorescence correlation spectroscopy (FCS), where tuning the observation spot size provides unprecedented detail[80]. Many organelles, macromolecular structures or larger complexes such as centrosomes, DNA replication foci, and chromosome domains are in the right size range of 100-200 nm to be resolved via SIM and benefit from the increased image contrast and imaging speed. Not surprisingly, SIM imaging has yielded insights into centrosome architecture and dynamics in various model organisms[81-84], actin-myosin network dynamics[85], DNA replication[86,87] and other aspects of nuclear organization[11,88].

However, although each SRM method may be better suited to certain applications over others, they still exhibit reasonable overlap. As more institutions and core facilities offer SRM techniques and cross-method expertise, researchers have additional options to validate SRM findings across different platforms, thereby preventing risks of misinterpreting artifacts for biological structures[21]. To guide researchers in their choice of SRM technique(s) Fig. 3 shows a decision-making scheme that is complemented by an overview of the most important features of various SRM techniques (Table 1).

Successful SRM is a multidimensional challenge that goes beyond the technicalities of the microscope itself (in fact, most SRM systems are not more difficult to operate than conventional systems). SRM also requires considerations on specimen or target characteristics, dye choice, labelling method, sample preparation, aberration correction, as well as downstream quality control, post-processing and quantitative analyses. Although this is true for any imaging approach, it becomes more critical with SRM as increased sensitivity and resolution tend to magnify potential problems. In addition, SMLM and STED benefit from basic knowledge of photophysical fluorophore properties and their optimization with proper buffer conditions or instrument settings. SIM and SMLM also require some computational post-processing knowledge, as well as recognizing and counteracting method-specific reconstruction artifacts. Community efforts have led to the development of open-source tools for unbiased quality control of SRM image data such as the SIMcheck[89] and NanoJ-SQUIRREL[90] plugins for ImageJ/Fiji, which include analyses such as Fourier ring correlation[91] to quantitatively assess the effective resolution. With resolution claims typically referring to optimal conditions imaging isolated beads or well-defined microtubules, the latter is also an important step towards standardizing the determination of effective resolutions in a given dataset[28,92]. Molecular nanoscopic rulers based on DNA origami are another useful tool towards this goal[93,94].

As with any technological advancement new users need to be prepared for the considerable effort required to adapt and optimize experimental design and sample preparation. In-depth protocols have meanwhile become available to guide users through these processes[18,27,95-98] and Box 2 provides a concise list of golden rules to successful SRM. Finally, with SRM systems increasingly being operated in core facilities, skilled experts stand ready to advise biologists in their research endeavours.

SRM as a tool to inform biology

The number of biology-driven publications that use SRM as a tool for discovery has increased significantly in recent years (Fig. 4). For instance, Lovelace and co-workers[99] used SIM and SMLM to show that beyond its known roles in cell junctions and angiogenesis[100], the Rho GTPase-activating protein ARHGAP18/SENEX also localizes in distinct cellular puncta that wrap around microtubules at regular intervals (Fig. 4a). Crittenden et al[101] used ExM to demonstrate that in the mammalian brain striosomal fibres are intertwined with the dopamine-containing dendrites of striatonigral fibres and form bouquet-like structures that target bundles of ventrally extending dopamine-containing dendrites and clusters of their parent nigral cell bodies (Fig. 4b). Through SRM approaches researchers are able to peer deeper into the cell's individual organelles. For instance, Maeshima and colleagues studied higher order chromatin structure and dynamics with live-cell SMLM[102]. By combining PALM and single nucleosome tracking, they demonstrated that nucleosomes form coherently moving compact domains of ~160 nm that are determined by combined cohesin and intra-nucleosome interactions (Fig. 4c). SRM also permitted the identification and quantification of

single DNA replicons at the cellular level ~50 years after their proposed existence[87] (Fig. 4d). In addition, using STED Große and colleagues showed that the pro-apoptotic Bax protein forms ring structures on the mitochondrial surface[103] (Fig. 4e) that correlate with Cytochrome C release and may be required for Bax's established role in mitochondrial outer membrane permeabilization. Numerous other publications have employed SRM to further biological understanding of centrosome structure and function[81,104], nuclear and chromatin organization[105-107], nuclear pore function[75], mitochondrial membrane protein organization[108], and liver cell fenestrations[109]. The potential of SRM to inform pathology analyses and routine clinical investigations has also started to become apparent[47].

Since no all-purpose SRM method is available, the use of complementary microscopy readouts is often advantageous to extract more information from the biological system. For example, by employing different conventional and SRM microscopy techniques, Fritzsche et al. highlighted previously unrecognised features of the actin cytoskeleton in T-cell activation[110]. Similarly, STED-based traction force microscopy provided cellular force maps with improved detail[111]. The combination of complementary SRM and EM techniques offers a powerful route to important structural and mechanistic insights. For instance, Jung et al. used SMLM in combination with variable angle TIRF, scanning and transmission EM to determine that T-cell receptors are highly localized on microvilli of T-cells, but rarely on the cell body[112]. Poulter and co-workers used EM, TIRF, SIM and dSTORM to unravel the structural organization and signalling pathways associated with actin nodule formation[113]. Separately, Guizetti et al. combined conventional live-cell, SIM and cryo-EM tomography to identify ESCRT-III dependent contractile helical filaments mediating cell abscission in dividing human cells[114].

These examples demonstrate that the capacity of SRM to resolve biological structures in great detail enables researchers to revisit and refine biological models the description of which might have been oversimplified or incomplete due to the restrictions of diffraction-limited lower resolution images. Consequently, SRM-based 'descriptive' research is becoming increasingly necessary alongside hypothesis-driven work if (patho)biology is to be better understood[115].

Conclusions and future directions

SRM techniques still require considerable expertise and training. As more research labs use SRM approaches, both benefits and limitations in their biological application are becoming more evident. Elucidating full biological complexity requires 3D SRM solutions that allow simultaneous acquisition of as many labels as possible with sufficient speed while also keeping photobleaching/-toxicity acceptably low, which is well beyond present capabilities. Nonetheless, current developments are striving to reduce the current constraints (Fig. 2). A key task is to improve SRM's live-cell imaging capabilities by increasing temporal resolution and lowering photon burden. Challenges include optimized sample preparation and labelling, further reducing phototoxicity, and adaptation to imaging deep inside tissue.

A major handicap of all far-field SRM methods is their susceptibility to aberrations, in particular when imaging deeper than ~10 µm, which impacts contrast and resolution. Hence, implementation of adaptive optics (AO) using deformable mirror devices to compensate for refractive index changes within the specimen is expected to become more widespread[116]. AO will not only allow deeper SRM imaging into (live) biological tissues and organisms, but will also alleviate the current requirements of manual aberration correction, and will significantly enhance resolution in the axial direction. Recent work impressively demonstrated AO-improved STED microscopy of

aberrating samples[117] as well as whole-cell SRM with AO-assisted opposing objective (4Pi) single molecule switching nanoscopy (W-4piSMSN) featuring isotropic resolution of 10-20 nm over a depth of several µm[118]. Imaging beyond 50 µm depth will require 2-photon implementations of SRM as shown in several proof of principle applications[8].

Another major obstacle, particularly for diffraction-unlimited SRM, is the much higher photon demand, both on the excitation (for inhibiting fluorescence, e.g. STED) and the detection side (for an accurate molecular localization, SMLM). This has been tackled by combining targeted and stochastic nanoscopy in an approach termed MINFLUX (single molecule localization with MINimal emission FLUXes), which increased localization accuracy to the low nm range at much reduced excitation powers and by minimizing photon output instead of maximizing it[6,119]. For volumetric live-cell imaging, significant progress has been made with the introduction of light-sheet approaches, which provides unprecedented temporal resolution. Current efforts are aiming to improve its diffraction-limited lateral resolution[42,43,120,121]. Alternatively, simultaneous multi-plane imaging using diffractive optics or prisms in combination with SRM modalities promises a significant increase in the acquisition speed[122,123]. Finally, the development of improved reversibly switchable proteins and dyes, will make non-linear SIM and RESOLFT a more widespread option to achieve sub-100-nm structural resolution with much reduced light intensities[124-126].

Correlative imaging is another promising approach. Correlative SRM and EM of cryo-immobilized samples (Cryo-CLEM) offer the advantage that they combine the specificity of single molecule detection with nm-resolution that EM affords, with the superior native state preservation of fast-frozen vitrified samples compared to chemical fixation[127-129]. Combination with other readouts (such as force, electrophysiology or mass spectrometry) enhances the information content of imaging experiments, and it will be interesting to develop such hybrid approaches to be more accessible for biology-driven applications. Furthermore, combining SRM with fluorescence spectroscopy techniques such as fluorescence recovery after photobleaching (FRAP)[130,131], Förster resonance energy transfer (FRET)[132,133], and FCS[134] will further expand its applications to the study of structural dynamics and molecular interactions in living cells.

Increasing the number of targets beyond the usual 2-4 channels is becoming increasingly feasible for fixed-cell SRM by using combinatorial labelling[135], spectral unmixing[136] and liquid handling together with DNA-PAINT[97] or single molecule RNA-FISH[137]. Automation of acquisition and data analysis including implementation of machine/deep learning[138,139] will further increase the throughput and depth of information extracted from super-resolution data. This approach should prove particularly beneficial for denoising image data, permitting the reduction of the excitation power (lower photon burden), reduction of the acquisition time per image (higher temporal resolution), or the extension of the total acquisition time. Similarly, it will enable the automation of several other tasks, such as image segmentation, registration, and analysis of image data[138-140].

Establishing SRM as a common tool for routine life science research applications will require a more ergonomic design with intuitive handling, automated system calibration, data acquisition and processing. Deeper integration with novel information technology and electronics engineering is necessary, also in terms of handling data, since SRM generates large-scale biological data-sets. An image repository that not only allows researchers to evaluate raw data, but also links imaging data to other resources such as genome and proteome databases, and mines the collective metadata would be extremely valuable. An initial step has recently been made with the introduction of the Image Data Resource[141].

The financial burden of SRM is an additional consideration. Most SRM systems are still fairly expensive and therefore often collated in microscopy core facilities. However, various SRM solutions have emerged that lower costs by reducing complexity and waiving certain functionalities. These include commercial SRM solutions as well as bespoke simplified microscope designs using low-cost off-the-shelf components[142-144], open-source software solutions, such as SRRF[39] and chip integration[145] for use on standard low-cost microscopes. ExM is another low-cost and low-threshold SRM option for fixed cell and tissue imaging[45-48] (Table 1).

To simplify experimentation and allow evaluation of whole (and ideally live) samples and cell populations, we need solutions that permit instant image reconstruction. For techniques such as SIM and SRRF live image reconstruction is becoming readily available. Additionally, developing SRM systems that are flexibly and modularly expandable with, for instance, optical tweezers, microinjection, or laser ablation systems would significantly lower the threshold for biologists to use this methodology[146].

These constrains should not deter biologists from adding SRM to their toolbox. With careful scrutiny, SRM offers the potential for substantial refinement of how we understand (patho)biology and the opportunity to make new discoveries even with regard to processes thought to be well understood. With SRM, the biologist can 'boldly go where no one has gone before', making the future of life science research brighter and crisper at super-resolution.

Acknowledgements

We apologize to the many researchers whose work we were unable to cite owing to space constraints. Furthermore, we thank Ian Dobbie, Christoffer Lagerholm and Justin Demmerle for valuable comments on the manuscript. L.S. is supported by the Wellcome Trust Strategic Award 107457 supporting advanced microscopy at Micron Oxford. L.S. and T.H. acknowledge support by the European Union's Horizon 2020 research and innovation program under the Marie Sklodowska-Curie Grant Agreement No. 766181. G.D. is supported with funding for External Collaborative Research. M.S. acknowledges support by the Deutsche Forschungsgemeinschaft (DFG) within the Collaborative Research Center 166 ReceptorLight (projects A04 and B04). C.E. acknowledges support by the Medical Research Council (grant number MC_UU_12010/unit programs G0902418 and MC_UU_12025, grant MR/K01577X/1), Wellcome Trust (grant 104924/14/Z/14 and Strategic Award 107457), DFG (Research unit FOR 1905), and Oxford internal funds (EPA Cephalosporin Fund and John Fell Fund).

References

1. Pawley, J.B. *Handbook of biological confocal microscopy*, Edn. third. (Springer US, New York; 2006).
2. Sauer, M. & Heilemann, M. Single-Molecule Localization Microscopy in eukaryotes. *Chem. Rev.* (2017).
3. Fornasiero, E.F. & Opazo, F. Super-resolution imaging for cell biologists: concepts, applications, current challenges and developments. *Bioessays* **37**, 436-451 (2015).
4. Turkowyd, B., Virant, D. & Endesfelder, U. From single molecules to life: microscopy at the nanoscale. *Anal. Bioanal. Chem.* **408**, 6885-6911 (2016).
5. Eggeling, C., Willig, K.I., Sahl, S.J. & Hell, S.W. Lens-based fluorescence nanoscopy. *Q. Rev. Biophys.* **48**, 178-243 (2015).
6. Sahl, S.J., Hell, S.W. & Jakobs, S. Fluorescence nanoscopy in cell biology. *Nat. Rev. Mol. Cell Biol.* **18**, 685-701 (2017).
7. Heintzmann, R. & Huser, T. Super-resolution Structured Illumination Microscopy. *Chem. Rev.* **117**, 13890-13908 (2017).
8. Wu, Y. & Shroff, H. Faster, sharper, and deeper: structured illumination microscopy for biological imaging. *Nature Methods*, in press (2018).
9. Gustafsson, M.G. *et al.* Three-dimensional resolution doubling in wide-field fluorescence microscopy by structured illumination. *Biophys. J.* **94**, 4957-4970 (2008).
10. Kner, P., Chhun, B.B., Griffis, E.R., Winoto, L. & Gustafsson, M.G. Super-resolution video microscopy of live cells by structured illumination. *Nat. Methods* **6**, 339-342 (2009).
11. Schermelleh, L. *et al.* Subdiffraction multicolor imaging of the nuclear periphery with 3D structured illumination microscopy. *Science* **320**, 1332-1336 (2008).
12. Muller, C.B. & Enderlein, J. Image scanning microscopy. *Phys. Rev. Lett.* **104**, 198101 (2010).
13. York, A.G. *et al.* Resolution doubling in live, multicellular organisms via multifocal structured illumination microscopy. *Nature Methods* **9**, 749-U167 (2012).
14. Schulz, O. *et al.* Resolution doubling in fluorescence microscopy with confocal spinning-disk image scanning microscopy. *Proceedings of the National Academy of Sciences of the United States of America* **110**, 21000-21005 (2013).
15. York, A.G. *et al.* Instant super-resolution imaging in live cells and embryos via analog image processing. *Nat. Methods* **10**, 1122-1126 (2013).
16. Shao, L., Kner, P., Rego, E.H. & Gustafsson, M.G. Super-resolution 3D microscopy of live whole cells using structured illumination. *Nat. Methods* **8**, 1044-1046 (2011).
17. Fiolka, R., Shao, L., Rego, E.H., Davidson, M.W. & Gustafsson, M.G. Time-lapse two-color 3D imaging of live cells with doubled resolution using structured illumination. *Proc. Natl. Acad. Sci. U.S.A.* **109**, 5311-5315 (2012).
18. Demmerle, J. *et al.* Strategic and practical guidelines for successful structured illumination microscopy. *Nat. Protoc.* **12**, 988-1010 (2017).
19. De Luca, G.M. *et al.* Re-scan confocal microscopy: scanning twice for better resolution. *Biomed. Opt. Express* **4**, 2644-2656 (2013).
20. Huang, X.S. *et al.* Fast, long-term, super-resolution imaging with Hessian structured illumination microscopy. *Nature Biotechnology* **36**, 451-+ (2018).
21. Wegel, E. *et al.* Imaging cellular structures in super-resolution with SIM, STED and Localisation Microscopy: A practical comparison. *Sci. Rep.* **6**, 27290 (2016).
22. Göttfert, F. *et al.* Coaligned dual-channel STED nanoscopy and molecular diffusion analysis at 20 nm resolution. *Biophys. J.* **105**, L01-03 (2013).
23. Bottanelli, F. *et al.* Two-colour live-cell nanoscale imaging of intracellular targets. *Nat. Commun.* **7**, 10778 (2016).
24. Urban, N.T., Willig, K.I., Hell, S.W. & Nagerl, U.V. STED nanoscopy of actin dynamics in synapses deep inside living brain slices. *Biophys. J.* **101**, 1277-1284 (2011).

25. Heine, J. *et al.* Adaptive-illumination STED nanoscopy. *Proc. Natl. Acad. Sci. U.S.A.* **114**, 9797-9802 (2017).
26. van de Linde, S., Heilemann, M. & Sauer, M. Live-cell super-resolution imaging with synthetic fluorophores. *Annu. Rev. Phys. Chem.* **63**, 519-540 (2012).
27. van de Linde, S. *et al.* Direct stochastic optical reconstruction microscopy with standard fluorescent probes. *Nat. Protoc.* **6**, 991-1009 (2011).
28. Demmerle, J., Wegel, E., Schermelleh, L. & Dobbie, I.M. Assessing resolution in super-resolution imaging. *Methods* **88**, 3-10 (2015).
29. Deschout, H. *et al.* Precisely and accurately localizing single emitters in fluorescence microscopy. *Nat. Methods* **11**, 253-266 (2014).
30. Baddeley, D. & Bewersdorf, J. Biological insight from super-resolution microscopy: What we can learn from localization-based images. *Annu. Rev. Biochem.* **87**, 965-989 (2018).
31. Tokunaga, M., Imamoto, N. & Sakata-Sogawa, K. Highly inclined thin illumination enables clear single-molecule imaging in cells. *Nat. Methods* **5**, 159-161 (2008).
32. Burgert, A., Letschert, S., Doose, S. & Sauer, M. Artifacts in single-molecule localization microscopy. *Histochem. Cell Biol.* **144**, 123-131 (2015).
33. Ishitsuka, Y., Nienhaus, K. & Nienhaus, G.U. Photoactivatable fluorescent proteins for super-resolution microscopy. *Methods Mol. Biol.* **1148**, 239-260 (2014).
34. Heilemann, M., Margeat, E., Kasper, R., Sauer, M. & Tinnefeld, P. Carbocyanine dyes as efficient reversible single-molecule optical switch. *J. Am. Chem. Soc.* **127**, 3801-3806 (2005).
35. Jones, S.A., Shim, S.H., He, J. & Zhuang, X. Fast, three-dimensional super-resolution imaging of live cells. *Nat. Methods* **8**, 499-508 (2011).
36. Wombacher, R. *et al.* Live-cell super-resolution imaging with trimethoprim conjugates. *Nat Methods* **7**, 717-719 (2010).
37. Takakura, H. *et al.* Long time-lapse nanoscopy with spontaneously blinking membrane probes. *Nat. Biotechnol.* **35**, 773-780 (2017).
38. Dertinger, T., Colyer, R., Iyer, G., Weiss, S. & Enderlein, J. Fast, background-free, 3D super-resolution optical fluctuation imaging (SOFI). *Proc. Natl. Acad. Sci. U.S.A.* **106**, 22287-22292 (2009).
39. Gustafsson, N. *et al.* Fast live-cell conventional fluorophore nanoscopy with ImageJ through super-resolution radial fluctuations. *Nat. Commun.* **7**, 12471 (2016).
40. Manley, S. *et al.* High-density mapping of single-molecule trajectories with photoactivated localization microscopy. *Nat. Methods* **5**, 155-157 (2008).
41. Keller, P.J., Schmidt, A.D., Wittbrodt, J. & Stelzer, E.H. Reconstruction of zebrafish early embryonic development by scanned light sheet microscopy. *Science* **322**, 1065-1069 (2008).
42. Planchon, T.A. *et al.* Rapid three-dimensional isotropic imaging of living cells using Bessel beam plane illumination. *Nat. Methods* **8**, 417-423 (2011).
43. Chen, B.C. *et al.* Lattice light-sheet microscopy: imaging molecules to embryos at high spatiotemporal resolution. *Science* **346**, 1257998 (2014).
44. Chang, B.J., Perez Meza, V.D. & Stelzer, E.H.K. csiLSFM combines light-sheet fluorescence microscopy and coherent structured illumination for a lateral resolution below 100 nm. *Proc. Natl. Acad. Sci. U.S.A.* **114**, 4869-4874 (2017).
45. Chen, F., Tillberg, P.W. & Boyden, E.S. Optical imaging. Expansion microscopy. *Science* **347**, 543-548 (2015).
46. Tillberg, P.W. *et al.* Protein-retention expansion microscopy of cells and tissues labeled using standard fluorescent proteins and antibodies. *Nat. Biotechnol.* **34**, 987-992 (2016).
47. Zhao, Y. *et al.* Nanoscale imaging of clinical specimens using pathology-optimized expansion microscopy. *Nat. Biotechnol.* **35**, 757-764 (2017).
48. Chang, J.B. *et al.* Iterative expansion microscopy. *Nat. Methods* **14**, 593-599 (2017).

49. Cahoon, C.K. *et al.* Superresolution expansion microscopy reveals the three-dimensional organization of the Drosophila synaptonemal complex. *Proceedings of the National Academy of Sciences of the United States of America* **114**, E6857-E6866 (2017).
50. Wang, Y.F. *et al.* Combined expansion microscopy with structured illumination microscopy for analyzing protein complexes. *Nat. Protoc.* **13**, 1869-1895 (2018).
51. Stelzer, E.H.K. Contrast, resolution, pixelation, dynamic range and signal-to-noise ratio: fundamental limits to resolution in fluorescence light microscopy. *J. Microsc.* **189**, 15-24 (1998).
52. Endesfelder, U. *et al.* Chemically induced photoswitching of fluorescent probes--a general concept for super-resolution microscopy. *Molecules* **16**, 3106-3118 (2011).
53. Fernandez-Suarez, M. & Ting, A.Y. Fluorescent probes for super-resolution imaging in living cells. *Nat. Rev. Mol. Cell Biol.* **9**, 929-943 (2008).
54. Yang, Z. *et al.* Super-resolution fluorescent materials: an insight into design and bioimaging applications. *Chem. Soc. Rev.* **45**, 4651-4667 (2016).
55. Uno, S.N. *et al.* A guide to use photocontrollable fluorescent proteins and synthetic smart fluorophores for nanoscopy. *Microscopy* **64**, 263-277 (2015).
56. Nienhaus, K. & Nienhaus, G.U. Fluorescent proteins for live-cell imaging with super-resolution. *Chem. Soc. Rev.* **43**, 1088-1106 (2014).
57. van de Linde, S. *et al.* Investigating cellular structures at the nanoscale with organic fluorophores. *Chem. Biol.* **20**, 8-18 (2013).
58. Stepanenko, O.V., Stepanenko, O.V., Kuznetsova, I.M., Verkhusha, V.V. & Turoverov, K.K. Beta-barrel scaffold of fluorescent proteins: folding, stability and role in chromophore formation. *Int. Rev. Cell Mol. Biol.* **302**, 221-278 (2013).
59. Lukinavicius, G. *et al.* A near-infrared fluorophore for live-cell super-resolution microscopy of cellular proteins. *Nat. Chem.* **5**, 132-139 (2013).
60. Lukinavicius, G. *et al.* Fluorogenic probes for live-cell imaging of the cytoskeleton. *Nat. Methods* **11**, 731-733 (2014).
61. Yan, Q. & Bruchez, M.P. Advances in chemical labeling of proteins in living cells. *Cell Tissue Res.* **360**, 179-194 (2015).
62. Grimm, J.B. *et al.* Bright photoactivatable fluorophores for single-molecule imaging. *Nat. Methods* **13**, 985-988 (2016).
63. Shim, S.H. *et al.* Super-resolution fluorescence imaging of organelles in live cells with photoswitchable membrane probes. *Proc. Natl. Acad. Sci. U.S.A.* **109**, 13978-13983 (2012).
64. Muyldermans, S. Nanobodies: natural single-domain antibodies. *Annu. Rev. Biochem.* **82**, 775-797 (2013).
65. Ries, J., Kaplan, C., Platonova, E., Eghlidi, H. & Ewers, H. A simple, versatile method for GFP-based super-resolution microscopy via nanobodies. *Nat. Methods* **9**, 582-584 (2012).
66. Mikhaylova, M. *et al.* Resolving bundled microtubules using anti-tubulin nanobodies. *Nat. Commun.* **6**, 7933 (2015).
67. Melak, M., Plessner, M. & Grosse, R. Actin visualization at a glance. *J. Cell Sci.* **130**, 525-530 (2017).
68. Simonson, P.D., Rothenberg, E. & Selvin, P.R. Single-molecule-based super-resolution images in the presence of multiple fluorophores. *Nano Lett.* **11**, 5090-5096 (2011).
69. Zhang, G., Zheng, S., Liu, H. & Chen, P.R. Illuminating biological processes through site-specific protein labeling. *Chem. Soc. Rev.* **44**, 3405-3417 (2015).
70. Stanly, T.A. *et al.* Critical importance of appropriate fixation conditions for faithful imaging of receptor microclusters. *Biol Open* **5**, 1343-1350 (2016).
71. Ehmann, N. *et al.* Quantitative super-resolution imaging of Bruchpilot distinguishes active zone states. *Nat. Commun.* **5**, 4650 (2014).
72. Jungmann, R. *et al.* Quantitative super-resolution imaging with qPAINT. *Nat. Methods* **13**, 439-442 (2016).

73. Waldchen, S., Lehmann, J., Klein, T., van de Linde, S. & Sauer, M. Light-induced cell damage in live-cell super-resolution microscopy. *Sci. Rep.* **5**, 15348 (2015).
74. Lando, D. *et al.* Quantitative single-molecule microscopy reveals that CENP-A(Cnp1) deposition occurs during G2 in fission yeast. *Open Biol.* **2**, 120078 (2012).
75. Loschberger, A. *et al.* Super-resolution imaging visualizes the eightfold symmetry of gp210 proteins around the nuclear pore complex and resolves the central channel with nanometer resolution. *J. Cell Sci.* **125**, 570-575 (2012).
76. Szymborska, A. *et al.* Nuclear pore scaffold structure analyzed by super-resolution microscopy and particle averaging. *Science* **341**, 655-658 (2013).
77. Westphal, V. *et al.* Video-rate far-field optical nanoscopy dissects synaptic vesicle movement. *Science* **320**, 246-249 (2008).
78. Galiani, S. *et al.* Super-resolution microscopy reveals compartmentalization of peroxisomal membrane proteins. *J. Biol. Chem.* **291**, 16948-16962 (2016).
79. Berning, S., Willig, K.I., Steffens, H., Dibaj, P. & Hell, S.W. Nanoscopy in a living mouse brain. *Science* **335**, 551 (2012).
80. Eggeling, C. *et al.* Direct observation of the nanoscale dynamics of membrane lipids in a living cell. *Nature* **457**, 1159-1162 (2009).
81. Sonnen, K.F., Schermelleh, L., Leonhardt, H. & Nigg, E.A. 3D-structured illumination microscopy provides novel insight into architecture of human centrosomes. *Biol. Open* **1**, 965-976 (2012).
82. Mennella, V. *et al.* Subdiffraction-resolution fluorescence microscopy reveals a domain of the centrosome critical for pericentriolar material organization. *Nat. Cell Biol.* **14**, 1159-1168 (2012).
83. Lawo, S., Hasegan, M., Gupta, G.D. & Pelletier, L. Subdiffraction imaging of centrosomes reveals higher-order organizational features of pericentriolar material. *Nat. Cell Biol.* **14**, 1148-1158 (2012).
84. Conduit, P.T. *et al.* A molecular mechanism of mitotic centrosome assembly in Drosophila. *Elife* **3**, e03399 (2014).
85. Burnette, D.T. *et al.* A contractile and counterbalancing adhesion system controls the 3D shape of crawling cells. *J. Cell Biol.* **205**, 83-96 (2014).
86. Baddeley, D. *et al.* Measurement of replication structures at the nanometer scale using super-resolution light microscopy. *Nucleic Acids Res.* **38**, e8 (2010).
87. Chagin, V.O. *et al.* 4D Visualization of replication foci in mammalian cells corresponding to individual replicons. *Nat. Commun.* **7**, 11231 (2016).
88. Smeets, D. *et al.* Three-dimensional super-resolution microscopy of the inactive X chromosome territory reveals a collapse of its active nuclear compartment harboring distinct Xist RNA foci. *Epigenetics Chromatin* **7**, 8 (2014).
89. Ball, G. *et al.* SIMcheck: A toolbox for successful super-resolution sructured illumination microscopy. *Sci. Rep.* **5**, 15915 (2015).
90. Culley, S. *et al.* Quantitative mapping and minimization of super-resolution optical imaging artifacts. *Nat Methods* **15**, 263-266 (2018).
91. Nieuwenhuizen, R.P. *et al.* Measuring image resolution in optical nanoscopy. *Nat. Methods* **10**, 557-562 (2013).
92. Tortarolo, G., Castello, M., Diaspro, A., Koho, S. & Vicidomini, G. Evaluating image resolution in stimulated emission depletion microscopy. *Optica* **5**, 32-35 (2018).
93. Steinhauer, C., Jungmann, R., Sobey, T.L., Simmel, F.C. & Tinnefeld, P. DNA Origami as a Nanoscopic Ruler for Super-Resolution Microscopy. *Angew. Chem. Int. Ed. Engl.* **48**, 8870-8873 (2009).
94. Schmied, J.J. *et al.* DNA origami-based standards for quantitative fluorescence microscopy. *Nat. Protoc.* **9**, 1367-1391 (2014).

95. Komis, G. *et al.* Superresolution live imaging of plant cells using structured illumination microscopy. *Nat. Protoc.* **10**, 1248-1263 (2015).
96. Kraus, F. *et al.* Quantitative 3D structured illumination microscopy of nuclear structures. *Nat. Protoc.* **12**, 1011-1028 (2017).
97. Schnitzbauer, J., Strauss, M.T., Schlichthaerle, T., Schueder, F. & Jungmann, R. Super-resolution microscopy with DNA-PAINT. *Nat. Protoc.* **12**, 1198-1228 (2017).
98. Gould, T.J., Verkhusha, V.V. & Hess, S.T. Imaging biological structures with fluorescence photoactivation localization microscopy. *Nat. Protoc.* **4**, 291-308 (2009).
99. Lovelace, M.D. *et al.* The RhoGAP protein ARHGAP18/SENEX localizes to microtubules and regulates their stability in endothelial cells. *Mol. Biol. Cell* **28**, 1066-1078 (2017).
100. Chang, G.H. *et al.* ARHGAP18: an endogenous inhibitor of angiogenesis, limiting tip formation and stabilizing junctions. *Small GTPases* **5**, 1-15 (2014).
101. Crittenden, J.R. *et al.* Striosome-dendron bouquets highlight a unique striatonigral circuit targeting dopamine-containing neurons. *Proc. Natl. Acad. Sci. U.S.A.* **113**, 11318-11323 (2016).
102. Nozaki, T. *et al.* Dynamic organization of chromatin domains revealed by super-resolution live-cell imaging. *Mol. Cell* **67**, 282-293 e287 (2017).
103. Große, L. *et al.* Bax assembles into large ring-like structures remodeling the mitochondrial outer membrane in apoptosis. *EMBO J.* **35**, 402-413 (2016).
104. Ramdas Nair, A. *et al.* The microcephaly-associated protein Wdr62/CG7337 is required to maintain centrosome asymmetry in Drosophila neuroblasts. *Cell Rep.* **14**, 1100-1113 (2016).
105. Boettiger, A.N. *et al.* Super-resolution imaging reveals distinct chromatin folding for different epigenetic states. *Nature* **529**, 418-422 (2016).
106. Cattoni, D.I. *et al.* Single-cell absolute contact probability detection reveals chromosomes are organized by multiple low-frequency yet specific interactions. *Nat. Commun.* **8**, 1753 (2017).
107. Ricci, M.A., Manzo, C., Garcia-Parajo, M.F., Lakadamyali, M. & Cosma, M.P. Chromatin fibers are formed by heterogeneous groups of nucleosomes in vivo. *Cell* **160**, 1145-1158 (2015).
108. Wurm, C.A. *et al.* Nanoscale distribution of mitochondrial import receptor Tom20 is adjusted to cellular conditions and exhibits an inner-cellular gradient. *Proc. Natl. Acad. Sci. U.S.A.* **108**, 13546-13551 (2011).
109. Mönkemoller, V., Oie, C., Hubner, W., Huser, T. & McCourt, P. Multimodal super-resolution optical microscopy visualizes the close connection between membrane and the cytoskeleton in liver sinusoidal endothelial cell fenestrations. *Sci. Rep.* **5**, 16279 (2015).
110. Fritzsche, M. *et al.* Cytoskeletal actin dynamics shape a ramifying actin network underpinning immunological synapse formation. *Sci. Adv.* **3**, e1603032 (2017).
111. Colin-York, H. *et al.* Super-Resolved Traction Force Microscopy (STFM). *Nano Lett.* **16**, 2633-2638 (2016).
112. Jung, Y. *et al.* Three-dimensional localization of T-cell receptors in relation to microvilli using a combination of superresolution microscopies. *Proc. Natl. Acad. Sci. U.S.A.* **113**, E5916-E5924 (2016).
113. Poulter, N.S. *et al.* Platelet actin nodules are podosome-like structures dependent on Wiskott-Aldrich syndrome protein and ARP2/3 complex. *Nat. Commun.* **6**, 7254 (2015).
114. Guizetti, J. *et al.* Cortical constriction during abscission involves helices of ESCRT-III-dependent filaments. *Science* **331**, 1616-1620 (2011).
115. Saka, S. & Rizzoli, S.O. Super-resolution imaging prompts re-thinking of cell biology mechanisms: selected cases using stimulated emission depletion microscopy. *Bioessays* **34**, 386-395 (2012).
116. Booth, M.J. Adaptive optical microscopy: the ongoing quest for a perfect image. *Light Sci. Appl.* **3**, e165 (2014).

117. Gould, T.J., Burke, D., Bewersdorf, J. & Booth, M.J. Adaptive optics enables 3D STED microscopy in aberrating specimens. *Opt. Express* **20**, 20998-21009 (2012).
118. Huang, F. *et al.* Ultra-High Resolution 3D Imaging of Whole Cells. *Cell* **166**, 1028-1040 (2016).
119. Balzarotti, F. *et al.* Nanometer resolution imaging and tracking of fluorescent molecules with minimal photon fluxes. *Science* **355**, 606-612 (2017).
120. Gao, L. *et al.* Noninvasive imaging beyond the diffraction limit of 3D dynamics in thickly fluorescent specimens. *Cell* **151**, 1370-1385 (2012).
121. Gustavsson, A.K., Petrov, P.N., Lee, M.Y., Shechtman, Y. & Moerner, W.E. 3D single-molecule super-resolution microscopy with a tilted light sheet. *Nat. Commun.* **9**, 123 (2018).
122. Geissbuehler, S. *et al.* Live-cell multiplane three-dimensional super-resolution optical fluctuation imaging. *Nat. Commun.* **5**, 5830 (2014).
123. Abrahamsson, S. *et al.* Fast multicolor 3D imaging using aberration-corrected multifocus microscopy. *Nat. Methods* **10**, 60-63 (2013).
124. Rego, E.H. *et al.* Nonlinear structured-illumination microscopy with a photoswitchable protein reveals cellular structures at 50-nm resolution. *Proc. Natl. Acad. Sci. U.S.A.* **109**, E135-143 (2012).
125. Chmyrov, A. *et al.* Nanoscopy with more than 100,000 'doughnuts'. *Nat. Methods* **10**, 737-740 (2013).
126. Chmyrov, A. *et al.* Achromatic light patterning and improved image reconstruction for parallelized RESOLFT nanoscopy. *Sci. Rep.* **7**, 44619 (2017).
127. Chang, Y.W. *et al.* Correlated cryogenic photoactivated localization microscopy and cryo-electron tomography. *Nat. Methods* **11**, 737-739 (2014).
128. Kaufmann, R. *et al.* Super-resolution microscopy using standard fluorescent proteins in intact cells under cryo-conditions. *Nano Lett.* **14**, 4171-4175 (2014).
129. Liu, B. *et al.* Three-dimensional super-resolution protein localization correlated with vitrified cellular context. *Sci. Rep.* **5**, 13017 (2015).
130. Conduit, P.T., Wainman, A., Novak, Z.A., Weil, T.T. & Raff, J.W. Re-examining the role of Drosophila Sas-4 in centrosome assembly using two-colour-3D-SIM FRAP. *Elife* **4** (2015).
131. Tonnesen, J., Katona, G., Rozsa, B. & Nagerl, U.V. Spine neck plasticity regulates compartmentalization of synapses. *Nat. Neurosci.* **17**, 678-685 (2014).
132. Deng, S. *et al.* Effects of donor and acceptor's fluorescence lifetimes on the method of applying Forster resonance energy transfer in STED microscopy. *J. Microsc.* **269**, 59-65 (2018).
133. Winckler, P. *et al.* Identification and super-resolution imaging of ligand-activated receptor dimers in live cells. *Sci. Rep.* **3**, 2387 (2013).
134. Honigmann, A. *et al.* Scanning STED-FCS reveals spatiotemporal heterogeneity of lipid interaction in the plasma membrane of living cells. *Nat. Commun.* **5**, 5412 (2014).
135. Lubeck, E. & Cai, L. Single-cell systems biology by super-resolution imaging and combinatorial labeling. *Nat. Methods* **9**, 743-748 (2012).
136. Valm, A.M. *et al.* Applying systems-level spectral imaging and analysis to reveal the organelle interactome. *Nature* **546**, 162-167 (2017).
137. Moffitt, J.R., Pandey, S., Boettiger, A.N., Wang, S. & Zhuang, X. Spatial organization shapes the turnover of a bacterial transcriptome. *Elife* **5** (2016).
138. Nehme, E., Weiss, L.E., Michaeli, T. & Shechtman, Y. Deep-STORM: Super resolution single molecule microscopy by deep learning. *arXiv*, 1801.09631v09632 (2018).
139. Ouyang, W., Aristov, A., Lelek, M., Hao, X. & Zimmer, C. Deep learning massively accelerates super-resolution localization microscopy. *Nat Biotechnol* **36**, 460-468 (2018).
140. Kraus, O.Z. *et al.* Automated analysis of high-content microscopy data with deep learning. *Mol. Syst. Biol.* **13**, 924 (2017).
141. Williams, E. *et al.* The Image Data Resource: A bioimage data integration and publication platform. *Nat. Methods* **14**, 775-781 (2017).

142. Ma, H., Fu, R., Xu, J. & Liu, Y. A simple and cost-effective setup for super-resolution localization microscopy. *Sci. Rep.* **7**, 1542 (2017).
143. Kwakwa, K. *et al.* easySTORM: a robust, lower-cost approach to localisation and TIRF microscopy. *J. Biophotonics* **9**, 948-957 (2016).
144. Holm, T. *et al.* A blueprint for cost-efficient localization microscopy. *ChemPhysChem* **15**, 651-654 (2014).
145. Diekmann, R. *et al.* Chip-based wide field-of-view nanoscopy. *Nat. Photonics* **11**, 322-+ (2017).
146. Diekmann, R. *et al.* Nanoscopy of bacterial cells immobilized by holographic optical tweezers. *Nat. Commun.* **7**, 13711 (2016).
147. Li, D. *et al.* Extended-resolution structured illumination imaging of endocytic and cytoskeletal dynamics. *Science* **349**, aab3500 (2015).
148. Hofmann, M., Eggeling, C., Jakobs, S. & Hell, S.W. Breaking the diffraction barrier in fluorescence microscopy at low light intensities by using reversibly photoswitchable proteins. *Proc. Natl. Acad. Sci. U.S.A.* **102**, 17565-17569 (2005).
149. Grotjohann, T. *et al.* Diffraction-unlimited all-optical imaging and writing with a photochromic GFP. *Nature* **478**, 204-208 (2011).
150. Holden, S.J., Uphoff, S. & Kapanidis, A.N. DAOSTORM: an algorithm for high-density super-resolution microscopy. *Nat. Methods* **8**, 279-280 (2011).
151. Marsh, R.J. *et al.* Artifact-free high-density localization microscopy analysis. *Nature Methods* (2018).
152. Huang, B., Wang, W., Bates, M. & Zhuang, X. Three-dimensional super-resolution imaging by stochastic optical reconstruction microscopy. *Science* **319**, 810-813 (2008).
153. Pavani, S.R. *et al.* Three-dimensional, single-molecule fluorescence imaging beyond the diffraction limit by using a double-helix point spread function. *Proc. Natl. Acad. Sci. U.S.A.* **106**, 2995-2999 (2009).
154. Juette, M.F. *et al.* Three-dimensional sub-100 nm resolution fluorescence microscopy of thick samples. *Nat. Methods* **5**, 527-529 (2008).
155. Schoen, I., Ries, J., Klotzsch, E., Ewers, H. & Vogel, V. Binding-activated localization microscopy of DNA structures. *Nano Lett.* **11**, 4008-4011 (2011).
156. Szczurek, A. *et al.* Imaging chromatin nanostructure with binding-activated localization microscopy based on DNA structure fluctuations. *Nucleic Acids Res.* **45**, e56 (2017).
157. Liu, W. *et al.* Breaking the Axial Diffraction Limit: A Guide to Axial Super-Resolution Fluorescence Microscopy. *Laser & Photonics Reviews* (2018).
158. Sheppard, C.J.R., Mehta, S.B. & Heintzmann, R. Superresolution by image scanning microscopy using pixel reassignment. *Opt. Lett.* **38**, 2889-2892 (2013).
159. Huff, J. The Airyscan detector from ZEISS: confocal imaging with improved signal-to-noise ratio and super-resolution. *Nat. Methods* **12** (2015).
160. Korobchevskaya, K., Colin-York, H., Lagerholm, B. & Fritzsche, M. Exploring the Potential of Airyscan Microscopy for Live Cell Imaging. *Photonics* **4**, 41 (2017).
161. Chozinski, T.J. *et al.* Expansion microscopy with conventional antibodies and fluorescent proteins. *Nat. Methods* **13**, 485-488 (2016).

Box 1: Super-resolution principles

Conventional far-field fluorescence microscopy operates in the resolution range of 200-300 nm laterally and 500-800 nm axially[16] limited by the wavelength of light (λ) and the NA of the objective lens.

SIM – super-resolution by interference pattern

SIM involves illuminating the focal plane in a stripe pattern generated by interfering laser beams with a minimum stripe distance close to the resolution limit. The pattern frequency interacts with otherwise non-resolvable 'high frequency' sample features, resulting in larger-scale interferences (Moiré effects) that can pass through the objective's aperture. This encoded information is imaged intermixed with the frequencies of the conventional wide-field image. To improve spatial resolution along all lateral directions a series of raw images is consecutively acquired with translationally phase-shifted and rotated stripes (Fig. 1d). Frequency-shifted information is then algorithmically decoded and reassembled in frequency space to reconstruct a contrast-enhanced image (or stack) with two-fold increased lateral and axial resolution[9,11]. Linear 3D SIM can achieve a wavelength-dependent resolution of 100-130 nm laterally and 300-400 nm axially. The lateral resolution of linear SIM can be improved to ~80 nm and applied to fast live-cell imaging when combined with TIRF and ultra-high NA (1.7) objectives[147]. Higher resolution can be realized by reducing stripe widths going into nonlinear regimes, for example by reversible photoswitching non-linear SIM (NL-SIM) or parallelized RESOLFT [124,125].

STED – target-based inhibition of fluorescence emission by stimulated emission

In standard STED the confocal excitation beam is overlaid by a depletion laser beam with at least one local intensity minimum (usually in the focal centre) to inhibit or deplete fluorescence emission, apart from the local intensity minimum. This restricts spontaneous fluorescence emission to that region and shapes the effective scanning spot size to sub-diffraction scales (Fig. 1f). RESOLFT employs such a fluorescence inhibition scheme through reversibly photoswitchable fluorescent labels [148,149]. Image acquisition by STED/RESOLFT can be accelerated using multiple scanning beams [5], whereas spatial resolution can be tuned by the intensity of the off-switching/depletion laser. Expert laboratories can reach 30-80 nm lateral resolution in fixed- and live-cell experiments, compared to 60-120 nm when using commercial systems with STED-optimized dyes.

SMLM – pointillist imaging by single molecule localization

In SMLM small subsets of individual emitters are randomly activated or switched on/off in consecutive acquisitions. If sparse enough to be identified as single molecule switching events, signals become spatiotemporally separated and are collected over several thousands of camera frames. Raw data are computationally processed to detect single molecules and determine their centre positions with nanometre precision dependent on the number of photons detected per individual emitter. These are finally assembled through superimposition into a single-plane binary image[2]. The localization precision of SMLM along the optical axis is limited by the focal depth of the image plane, even when using multi-emitter fitting methods[150] or separating dense fluorophore locations based on their emission rate[151]. It can be improved to the sub-100-nm-range in most cases at the expense of lateral accuracy by introducing astigmatic [152] or helical [153] optical distortions, or by bi-plane detection [154]. The localization precision is usually expressed as a 1-σ error. The spatial

resolution can be estimated by the full width at half-maximum (FWHM) of the localization errors distribution of $\Delta x \approx 2.35\sigma$. Current SMLM approaches differ primarily in how on/off switching is achieved: (f)PALM utilizes photoactivation, STORM and dSTORM use photoswitching of activator and reporter dye-pairs or conventional fluorescent probes in the presence of thiols to transfer dyes to long-lived off-states, respectively, and (f)BALM ((fluctuation-assisted) binding-activated localization microscopy) uses binding and fluorescence activation of specific dyes [155,156]. DNA-PAINT/Exchange-PAINT [71,72] utilizes transient oligonucleotide hybridization opening new possibilities for multiplexed SMLM.

4Pi, I5M, iPALM, isoSTED - interferometric approaches to increase axial resolution

The first SRM realisations did not address the lateral resolution limit, but rather the apparent anisotropy of the resolution along the optical axis. This was achieved by using illumination through opposing lenses in a confocal (4Pi microscopy) or a widefield setup (I5M). Such interferometric setups were later combined with lateral SRM techniques, for example in iPALM or isoSTED[157], however their complexity and difficult alignment have limited their widespread use.

Box 2: The golden rules of SRM

1) *Focus on experimental design:* Is SRM essential to answer the biological question, or would conventional confocal or wide-field imaging suffice? Is high throughput or live-cell imaging necessary and if yes, can loss of resolution be afforded? Consider all aspects of experimental design, including sample thickness and required depth of imaging, sample preparation and labelling strategy, system alignment, acquisition parameters, reconstruction settings, data quality control, channel registration, quantification and data interpretation. Dedicate appropriate experiment planning time, seek advice, and put highest effort in generating best-quality samples.

2) *Specificity matters:* Unspecific labelling reduces contrast and generates false positives. To ensure the specificity of any label it is important to cross validate, e.g. by comparing antibody labelling to a genetic fusion protein.

3) *Contrast is key:* System alignment, fluorescence labelling, imaging settings and out-of-focus blur can affect image contrast. Imaging small and isolated objects with little out-of-focus blur requires less dynamic range. Conversely extended and more densely packed objects or structures, with high levels of out-of-focus light require high dynamic range to generate sufficient contrast.

4) *Reduce background:* Brighter is not automatically better if the background is also increased. A single fluorescing molecule generates enough photons to be detected, if background is low. Ideally, a field of view should contain some background areas, with grey levels close to the detection noise. Avoid potential auto-fluorescence of the embedding medium and thoroughly wash to remove unbound fluorescence labelling agent.

5) *Be clean*: Dust and dirt scatter light and affect the illumination quality and detection efficiency. Clean sample and objective before and after imaging. Avoid contamination of the immersion medium.

6) *Correct for spherical aberration by immersion medium choice or correction collar setting:* When selecting the refractive index of the immersion medium consider the temperature, desired colour and depth optimum, coverslip thickness and refractive index mismatches between immersion medium, embedding medium and specimen. Use immersion objectives to minimize refractive index mismatch when imaging deeper or live specimen[18].

7) *Match optical transfer functions (OTFs) with imaging conditions:* In interference-based SIM and deconvolution, if the sample in the depth of interest, with the specific imaging conditions and wavelength used contains spherical aberration, then reconstruction with an 'aberration-free' OTF will lead to artifacts. This can be minimized if the corresponding OTF encodes for the same level of spherical aberration (see rule 6). For multicolour applications, always use colour-specific measured OTFs acquired with the same index oil. This ensures that unavoidable wavelength-specific deviations in spherical aberrations are encoded in the OTFs.

8) *If imaging in 3D, register 3D:* To determine channel registration parameters in x, y and z for multi-camera systems, use 3D multispectral beads or biological 3D calibration samples[96], or add gold fiducials.

9) *Beware of drift:* To avoid artifacts ensure that mechanical components and ambient temperature are stable. For live-cell acquisitions, consider motion blur and adjust acquisition speed and intervals appropriately.

10) *Think of controls:* Start imaging with a reference sample and proven microscope settings to exclude technical issues. Consider testing sample quality by conventional imaging first. If possible, cross-validate findings with different (SRM) methods and apply appropriate controls throughout the imaging workflow.

11) *Balance dynamic range versus photobleaching:* Determine a sufficiently high dynamic range for good contrast, while keeping photobleaching over the acquisition tolerable.

12) *Spend your photon budget wisely:* Increasing spatial resolution requires higher light doses, longer acquisition time and reduced live-cell capability. Imaging multiple time points requires trade-offs in other areas, e.g. z-height and number of colour channels (Fig. 2).

13) *Emphasize quality and artefact controls:* If applicable, perform objective data quality control using SIMcheck and/or NanoJ-SQUIRREL ImageJ plugins [89,90]. If possible, confirm effective resolution in your data (e.g. by Fourier ring correlation[91]), and do not rely on best values from literature that are achievable in ideal conditions.

14) *Image processing improvements do not equate to information content improvements:* Image processing can remove background and smoothen the signal, which seems to make shot noise disappear. However, removal of noise and background image does not necessarily reflect an artefact-free image and may not represent the real structure.

Table 1| **Overview of super-resolution microscopy techniques currently (commercially) available for life scientists.**

	Method	Principle-Detector	3D res./ stack	2-color/ multi-colour	Live cell	Ease of use	Costs	Adv. mode	Sample prep.	Thick >20µm	Special probes	Merits	Disadvantages	Refs.
SR-SIM Point-scanning SIM	**Re-scan**	Single-point scanning - Camera	-/✓	✓/✓	(✓)	🟩	$	FRET[b]	🟩	✓	-	• No more difficult than confocal • 1 fps @ 512x512 pixel • Cost efficient • Standard sample preparation • Upgrade of existing equipment possible	• Limited resolution improvement (1.4-fold lateral, ~170 nm @ ex. 488nm)	19
	Airyscan	Single-point scanning - Photo-detector array	✓/✓	✓/✓	✓	🟩	$$	FCS FRET FRAP	🟩	✓	-	• No more difficult to use than confocal • Standard sample preparation • Faster live cell option • Improved SNR	• Limited resolution improvement (up to max 1.7-fold in x,y and z) • Rel. slow acquisition in high-resolution mode • Requires correct Airyscan filtering	158-160
	iSIM	Multi-point scanning - Camera	✓/✓	✓/✓	✓	🟩	$$		🟩	✓	-	• No more difficult to use than confocal • Standard sample preparation • High sensitivity • Relative high acquisition speed	• Limited resolution improvement (1.7-fold in x,y and z) • Optional iterative deconvolution for best quality.	14,15
Interference-based	**2D/ 3D SIM**	Wide-field (TIRF) - Camera	✓/✓	✓/✓[a]	✓[b]	🟨	$$$	FRAP	🟨	-	-	• True multicolour (3-4) • Fast acquisition of larger volumes • Linear reconstruction process • Superior high-frequency information throughput • Very high contrast increase	• Expensive equipment • Not for thick samples (>20 µm)[c] • Post-processing needed • Prone to reconstruction artifacts	7,9,18,147
	STED	Point scanning - Photo-detector	(✓)/✓	✓/-	-/✓[d]	🟨	$$$ /$	FCS FRAP	🟩	✓	✓	• Very high 2D-, high 3D-resolution • Direct super-resolved images • Improved live cell capabilities (DyMIN STED) • Low cost upgrade option with reduced system complexity and capabilities available (*STEDYCON*)	• Slow acquisition for larger area • Limited multicolour choice • Expensive equipment • High peak light intensities -> Prone to photodamage • Signal-to-noise limited due to small detection volume	5

RESOLFT	STED, SIM	✓/-	-/-	✓	🟨	$$$	-	🟧	-	✓	• Diffraction unlimited resolution • Relative low light intensities • Live cell imaging possible	• Requires specific reversible switchable dyes/FP tags • Routinely single-colour only	147-149
SMLM	Wide-field TIRF HILO - Camera	✓/-	✓/-	-	🟨	$$	FRET[e]	🟧	-	✓	• Very high resolution • Single molecule detection • Relative simple microscope setup • Can be combined with TIRF and inclined illumination (HILO) • Quantification of protein numbers • Upgrade solution for existing setups to enable extended 3D localization using PSF engineering (e.g. Double Helix)	• Special buffers/probes required • Not for thick samples (< 10 µm) • Slow acquisition imaging • Limited 3D (no sectioning) • Advanced postprocessing needed • Virtual super-resolved image • Prone to reconstruction artifacts • Structural resolution labelling density dependent	72,97
SOFI/ SRRF	Algorithm	✓	✓/-	✓	🟨	$	✓	🟨	-	(✓)	• Can be used with all standard imaging modalities • Very cost efficient • Rel. low illumination possible → live cell imaging capable	• Only moderate resolution increase	38,39
LLS	Light-sheet & SIM - Camera	✓	✓[e]/-	✓	🟧	$$$	FRET	🟨	✓	-	• Fast live whole cell imaging • High contrast • Low photo-toxicity/bleaching • Thick samples up to 50 µm • Volumetric field of view: ~50×50×50 µm	• Limited resolution improvement • Expensive and difficult to maintain equipment • Transparent samples required	43
ExM	Sample prep. kit [f]	✓	✓/✓	-	🟩	$-$$		🟨	✓	(✓)	• Very cost efficient • Requires no special equipment • Resolution increase 4.5-fold (ExM)	• Fixed samples only • Requires morphology checks	45,48,161

[a] Multicolour imaging is performed sequentially; [b] Fast SIM, requires system equipped with Blaze unit (*GE OMX*) or spatial light modulator for pattern generation; [c] Deeper imaging requires silicone immersion objective; [d] new STED implementations significantly reduce irradiation for improved live cell imaging capability; [e] Not all SMLM variants; [f] Kit contains the fixatives and the polymer swelling matrix; $: Low cost; $$: Moderate cost; $$$: High cost; ExM: Expansion microscopy; HILO: Highly inclined and laminated optical sheet.

Figure Legends

Figure 1| **Basic principles of SRM.** Simplified light paths of common conventional (**a-c**) and super-resolution microscopy techniques (**d-h**) as described in the main text and Box 1. For better comparison all techniques are displayed in upright configuration, even though inverted configurations are more common, particular for TIRF, SIM and SMLM systems. Note the relationships between illumination of the pupil plane (back focal plane) and the corresponding illumination of the object plane (effectively the Fourier transform of the pupil plane). Wide-field illumination (**a**) is achieved by focussing the excitation light to a single spot in the centre of the pupil plane. In TIRF (**b**) the spot is shifted to the edge of the pupil plane, so that the light beam encounters the coverslip interface at a supercritical angle from the optical axis generating a rapidly decaying excitation beam close to the coverslip surface. In contrast, in confocal microscopy (**c**) the pupil plane is filled, which generates a focussed spot in the image plane to be scanned across the field-of view. Accordingly, the emitted light is either detected simultaneously using a camera (typically EMCCD or sCMOS) or point-by-point using photodetectors. Advanced imaging methods shown in **d-h** are derived from conventional configurations as indicated by the grey arrows. Dotted arrows indicate possible combinations between advanced techniques (currently limited to specialised labs). Round inset magnifications illustrate the direction of the excitation wavefronts (blue lines and arrows) and the direction of the emission (green arrows). For space constraints, RESOLFT, ExM and the LLS excitation light path are not shown in detail. Properties of techniques written in bold black are detailed in Fig. 2.

Figure 2| **Inherent trade-offs in SRM.** Diagram illustrating the main properties of commercially-available SRM and conventional microscopy techniques. From top left: Sample and microscope specific properties determine the overall limited photon budget (i.e. the number of target-specific photons collected from a fluorescent sample) available to achieve the four core objectives of biological imaging: spatial resolution, multicolour and 3D context, acquisition speed, and low photodamage. Improvement in one area inevitably implies compromises in others. Achievable contrast, optical aberrations, detector properties and the efficiency of resolution to illumination dose increase are specific limiting factors. Ovals and rectangles in the left panel indicate each technique's resolution in x, y- and z-dimension in optimal conditions. TIRF implementations can only image a thin ≤0.2 µm layer close to the coverslip. Factors such as fluorophore orientation, local refractive index variations, flat-field camera quality, local aberrations, and statistical selection bias can also negatively affect the final image quality and the effectively achievable resolution. Vertical diagrams indicate typical ranges of imaging depth, acquisition speed and illumination intensity for each technique. SMLM acquisitions are typically restricted to a single plane and similar to SIM lose quality when imaging deeper than a typical adherent cell (±10 µm). All other laser scanning- and light sheet-based techniques are less susceptible to degradation when imaging deeper, e.g. into tissue. Acquisition speeds are estimated based on the lowest exposure times required to imaging a single plane (SMLM, TIRF) or a volume of a typical mammalian cell with comparable signal-to-noise-ratio. The illumination light intensity critically contributes to the total light dosage (illumination intensity/peak intensity × exposure/pixel dwell time × number of exposures/averaging), which is inversely correlated with the technique's live-cell imaging capability.

Figure 3| **Decision tree for selecting SRM techniques.** The demands of the biological question should be the main determinant for the method of choice. If it requires live-cell imaging, the obtainable resolution is limited and imaging speed becomes the main criterium. In this case exposure times and photon burden should be considered in order to limit oxidative stress and photobleaching. If answering it requires sub-100-nm resolution and can be addressed in fixed-cell applications, diffraction unlimited techniques, such as SMLM and STED, are preferable. The ease of use of a particular technique determines its suitability for high sample throughput or use in a routine setting. Depending on the number of events that need to be acquired or the dynamics of the biological process, acquisition speed and the minimal resolution needed to answer the question are major criteria.

Figure 4| **Application examples of SRM to inform biology.** (**a**) SRM imaging reveals that ARHGAP18/SENEX localizes to microtubules in cultured endothelial cells. Wide-field (WF) images are shown at the top right. SIM visualises distinct puncta on tubulin (white arrows) that are not resolvable in the WF images. SMLM shows a distinct distribution even within the puncta. Images reproduced from Ref [99] with permission © 2017: American Society for Cell Biology. (**b**) Confocal and Expansion microscopy (ExM) images of mouse triosome–dendron bouquets. Confocal: *Substantia nigra pars compacta* (SNc) neurons and their ventrally extending dendrites (red); striosomal axons (green); tightly entwined striosomal and dopaminergic fibres in dendrons (yellow). ExM imaging of the bouquet resolves individual striosomal fibers (green) and dendrites (red) in a longitudinal view (middle) and in cross-sections at three levels (bottom). The top scale bar indicates the dimension of the unexpanded tissue, whereas other scale bars indicate the dimension of the expanded tissue. Reproduced from Ref [101] with permission © 2016: National Academy of Sciences of the United States of America. (**c**) Visualization of chromatin domain dynamics with live-cell PALM in HeLa cells. Middle: The chromatin heatmap indicates local movements in nm/50 ms time interval (right), with magnified insets the boxed regions (left) revealing significant differences in domain mobility. Reproduced from Ref [102] with permission © 2017: Elsevier Inc. (**d**) Replication sites imaged with fluorescence microscopy at different levels of resolution in the mammalian nucleus. Only SRM shows that replication sites correspond to individual replicons. Reproduced from Ref [87] with permission © 2016: SpringerNature. (**e**) Confocal image of an apoptotic U2OS cell labelled with Bax (green) and Tom22 (red). STED imaging of the Bax signal reveals that Bax forms a ring on apoptotic mitochondria within an area that is devoid of the mitochondrial outer membrane protein Tom22. Reproduced from Ref [103] with permission © 2016: The EMBO Journal.

Figure 1

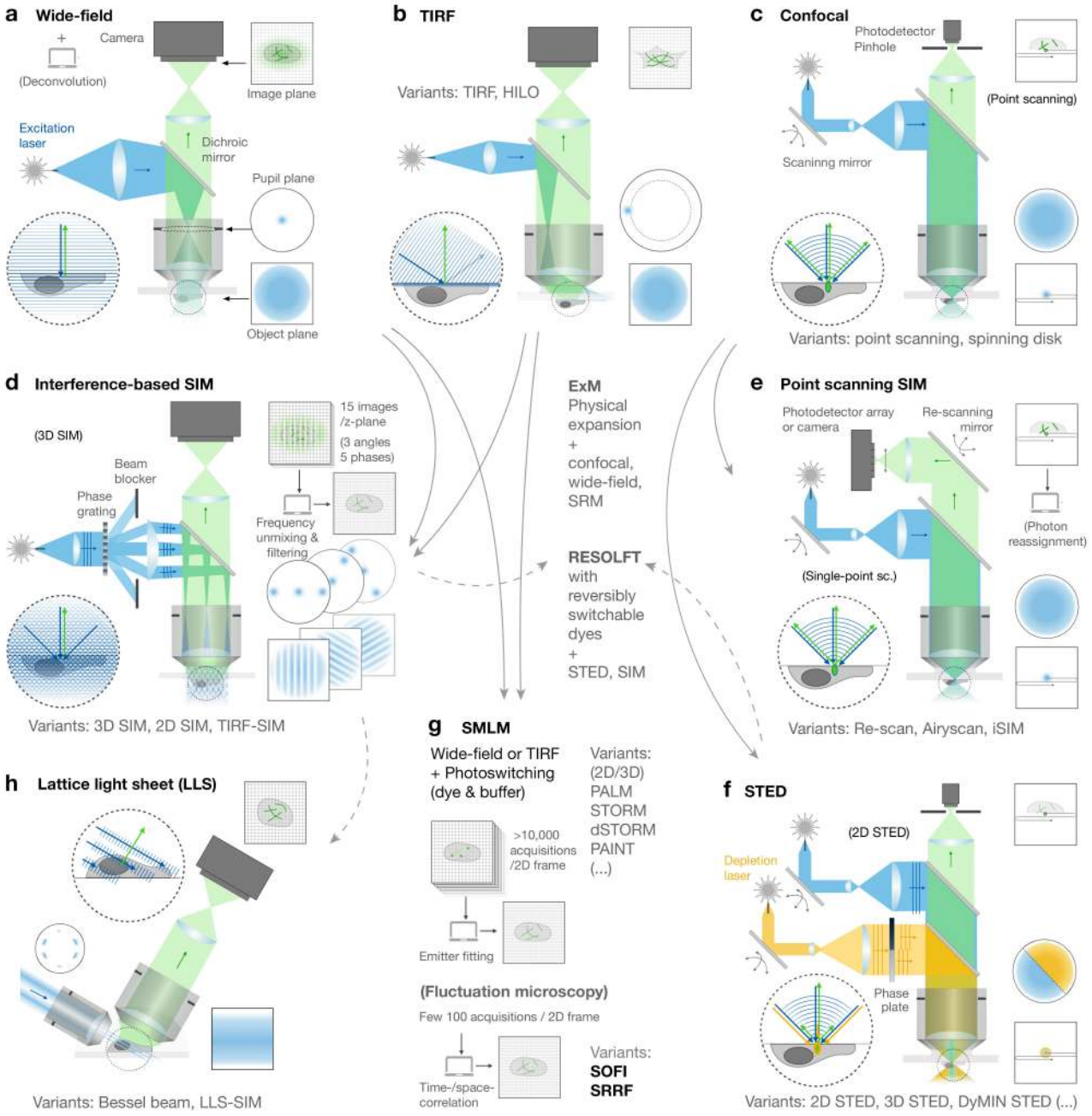
a Wide-field
Camera
(Deconvolution)
Image plane
Excitation laser
Dichroic mirror
Pupil plane
Object plane
b TIRF
Variants: TIRF, HILO
c Confocal
Photodetector
Pinhole
(Point scanning)
Scaninng mirror
Variants: point scanning, spinning disk
d Interference-based SIM
(3D SIM)
Beam blocker
Phase grating
15 images /z-plane
(3 angles 5 phases)
Frequency unmixing & filtering
Variants: 3D SIM, 2D SIM, TIRF-SIM
ExM
Physical expansion + confocal, wide-field, SRM
RESOLFT
with reversibly switchable dyes + STED, SIM
e Point scanning SIM
Photodetector array or camera
Re-scanning mirror
(Photon reassignment)
(Single-point sc.)
Variants: Re-scan, Airyscan, iSIM
g SMLM
Wide-field or TIRF + Photoswitching (dye & buffer)
Variants: (2D/3D) PALM STORM dSTORM PAINT (...)
>10,000 acquisitions /2D frame
Emitter fitting
(Fluctuation microscopy)
Few 100 acquisitions / 2D frame
Time-/space-correlation
Variants: SOFI SRRF
h Lattice light sheet (LLS)
Variants: Bessel beam, LLS-SIM
f STED
(2D STED)
Depletion laser
Phase plate
Variants: 2D STED, 3D STED, DyMIN STED (...)

Figure 2

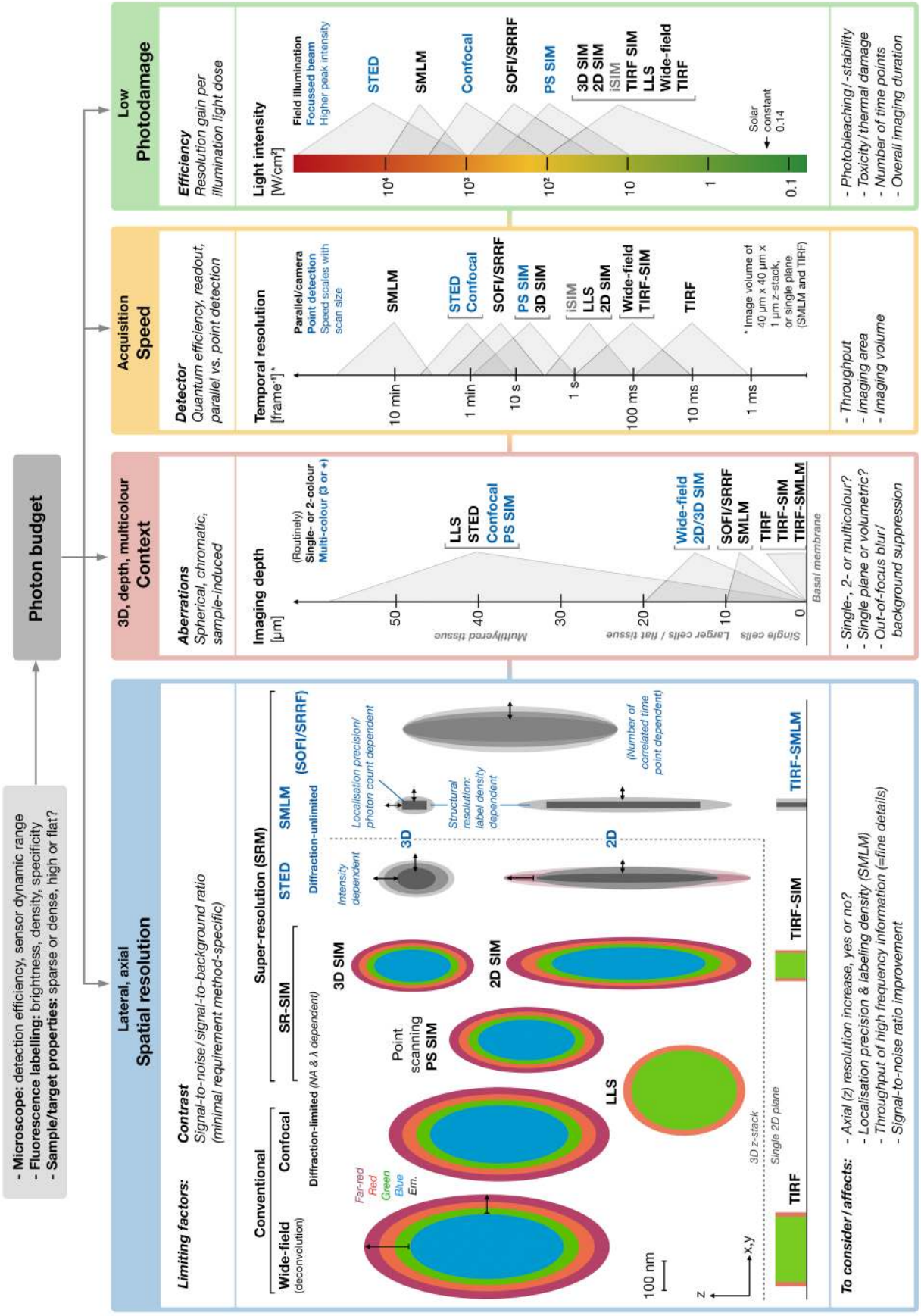
- Microscope: detection efficiency, sensor dynamic range
- Fluorescence labelling: brightness, density, specificity
- Sample/target properties: sparse or dense, high or flat?
Photon budget
Lateral, axial
Spatial resolution
Limiting factors:
Contrast
Signal-to-noise / signal-to-background ratio
(minimal requirement method-specific)
Conventional
Wide-field
(deconvolution)
Confocal
Diffraction-limited (NA & λ dependent)
Super-resolution (SRM)
SR-SIM
STED
SMLM
(SOFI/SRRF)
Diffraction-unlimited
3D SIM
2D SIM
Point scanning PS SIM
LLS
TIRF
TIRF-SIM
TIRF-SMLM
Intensity dependent
Localisation precision/ photon count dependent
Structural resolution: label density dependent
(Number of correlated time point dependent)
3D
2D
Far-red
Red
Green
Blue
Em.
100 nm
x,y
z
3D z-stack
Single 2D plane
To consider / affects:
- Axial (z) resolution increase, yes or no?
- Localisation precision & labeling density (SMLM)
- Throughput of high frequency information (=fine details)
- Signal-to-noise ratio improvement
3D, depth, multicolour
Context
Aberrations
Spherical, chromatic, sample-induced
Imaging depth
[µm]
(Routinely)
Single- or 2-colour
Multi-colour (3 or +)
LLS
STED
Confocal
PS SIM
Wide-field
2D/3D SIM
SOFI/SRRF
SMLM
TIRF
TIRF-SIM
TIRF-SMLM
Basal membrane
Single cells
Larger cells / flat tissue
Multilayered tissue
50
40
30
20
10
0
- Single-, 2- or multicolour?
- Single plane or volumetric?
- Out-of-focus blur/ background suppression
Acquisition
Speed
Detector
Quantum efficiency, readout, parallel vs. point detection
Temporal resolution
[frame-1] *
Parallel/camera
Point detection
Speed scales with scan size
SMLM
STED
Confocal
SOFI/SRRF
PS SIM
3D SIM
iSIM
LLS
2D SIM
Wide-field
TIRF-SIM
TIRF
10 min
1 min
10 s
1 s
100 ms
10 ms
1 ms
* Image volume of 40 µm x 40 µm x 1 µm z-stack, or single plane (SMLM and TIRF)
- Throughput
- Imaging area
- Imaging volume
Low
Photodamage
Efficiency
Resolution gain per illumination light dose
Light intensity
[W/cm²]
Field illumination
Focussed beam
Higher peak intensity
STED
SMLM
Confocal
SOFI/SRRF
PS SIM
3D SIM
2D SIM
iSIM
TIRF SIM
LLS
Wide-field
TIRF
Solar constant 0.14
10⁴
10³
10²
10
1
0.1
- Photobleaching / -stability
- Toxicity / thermal damage
- Number of time points
- Overall imaging duration

Figure 3

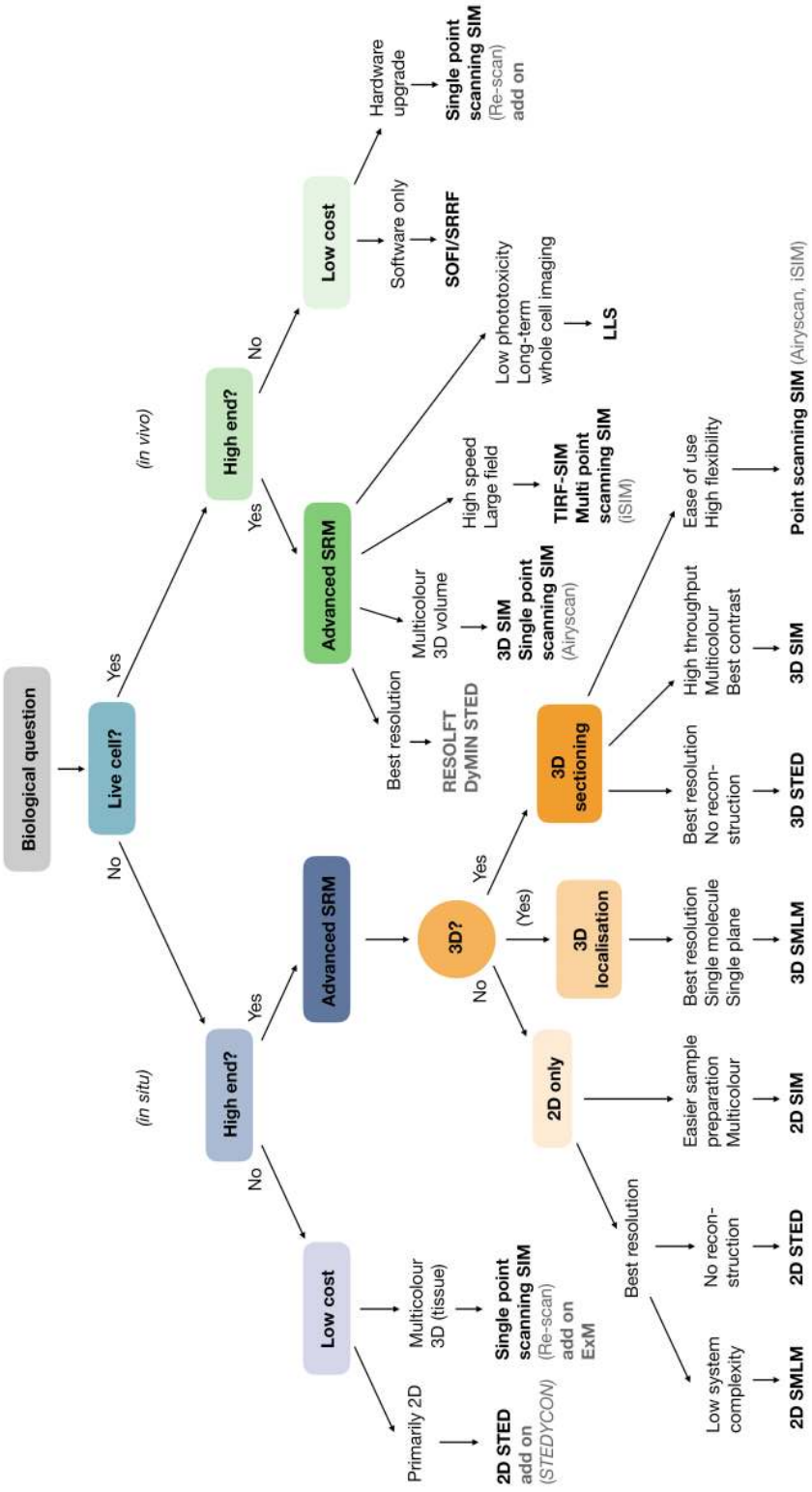
Biological question
Live cell?
Yes
No
(in vivo)
(in situ)
High end?
Yes
No
Low cost
Advanced SRM
Hardware upgrade
Single point scanning SIM (Re-scan) add on
Software only
SOFI/SRRF
Best resolution
RESOLFT DyMIN STED
Multicolour 3D volume
3D SIM Single point scanning SIM (Airyscan)
High speed Large field
TIRF-SIM Multi point scanning SIM (iSIM)
Low phototoxicity Long-term whole cell imaging
LLS
3D?
(Yes)
No
3D sectioning
3D localisation
2D only
Best resolution No recon-struction
3D STED
High throughput Multicolour Best contrast
3D SIM
Ease of use High flexibility
Point scanning SIM (Airyscan, iSIM)
Best resolution Single molecule Single plane
3D SMLM
Easier sample preparation Multicolour
2D SIM
Best resolution
No recon-struction
2D STED
Low system complexity
2D SMLM
Primarily 2D
2D STED add on (STEDYCON)
Multicolour 3D (tissue)
Single point scanning SIM (Re-scan) add on ExM

Figure 4

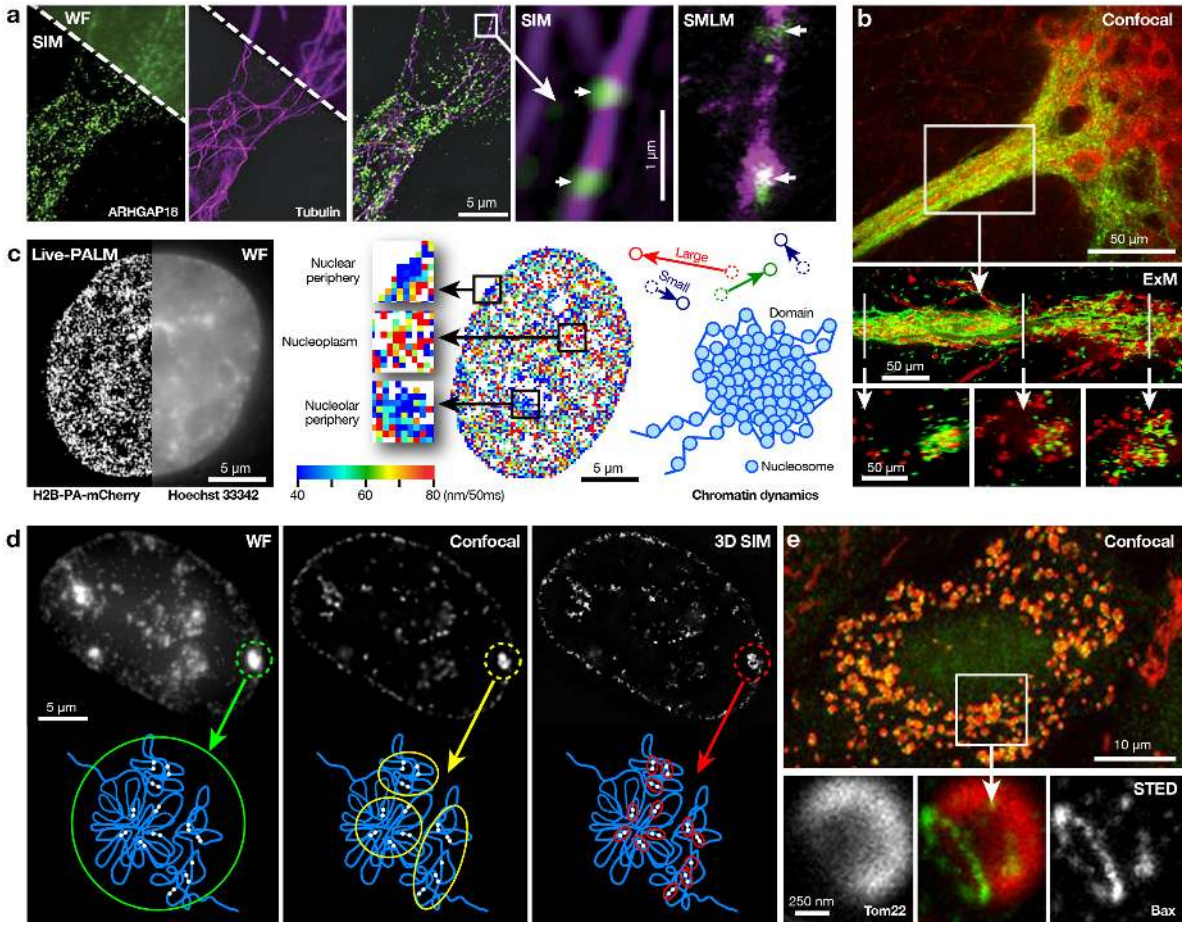
a
WF
SIM
ARHGAP18
Tubulin
5 μm
SIM
1 μm
SMLM
b
Confocal
50 μm
ExM
50 μm
50 μm
c
Live-PALM
WF
5 μm
H2B-PA-mCherry
Hoechst 33342
Nuclear periphery
Nucleoplasm
Nucleolar periphery
40
60
80 (nm/50ms)
5 μm
Large
Small
Domain
Nucleosome
Chromatin dynamics
d
WF
5 μm
Confocal
3D SIM
e
Confocal
10 μm
STED
250 nm
Tom22
Bax